Grid Diagnostics: Monitoring Cable Aging Using Power Line Transmission

Lena Förstel and Lutz Lampe
University of British Columbia, Vancouver, BC, Canada

***Abstract*—Power line communication (PLC) operates on the power line infrastructure to enable data exchange between terminals. In doing so, PLC modems transmit relatively high-frequency and broadband signals through the grid. It is easy to see that the distortion of these signals provides information about the physical properties of grid components affecting the transmission. This is the basis for performing grid diagnostics as a secondary or even as the primary application of PLC. In this paper, we investigate the question whether broadband PLC can be used to detect cable aging, which is an important task for grid maintenance. We apply a physical model for the degradation of serviced-aged cables due to water treeing, and investigate its detectability using channel frequency responses as experienced by PLC signals. The latter is illustrated through the study of frequency-response variations in a small power line network and accomplished through classification with a support vector machine. Our numerical results are encouraging in that some water-treeing degraded and intact cables can be differentiated.**

***Index Terms*—Grid diagnostics, cable aging, power line communications (PLC), transmission line theory**

I. Introduction

Power line communication (PLC) has experienced significant advances over the past 10 to 15 years in terms of introducing latest communication and signal processing techniques into PLC standards and systems [1]. With the rise of smart grids, PLC research has also started to focus on problems related to grid communications, which is the original application domain of PLC. In fact, PLC is a dominating solution for smart metering with a concentration of deployments and trials in Europe. While other technologies can be used to accomplish smart grid communication tasks, PLC is unique in that its signals travel through the power line infrastructure. This in turn enables inference about the infrastructure properties, i.e., grid diagnostics.

PLC for grid diagnostics is a relatively unexplored field. Previous works include the transmission of relatively short pulses for fault detection [2], [3], the use of broadband signals for detecting the grid topology [4], [5], and the testing of cable conditions using frequency response measurements [6], [7] and broadband impedance-spectroscopy [8]. In this paper, we concentrate on the problem of power cable condition monitoring using broadband PLC, similar to [6]–[8].

The monitoring of cable conditions is an important component in detecting a problem due to cable aging before a fault occurs or a functionality has been notably compromised. To this end, online testing methods are critical to assist the decision process. Our vision of PLC enabled online monitoring is that in parallel to the data transmission, the broadband signals exchanged between modems of a PLC network are also exploited for real-time inference on the cable infrastructure. For cable aging, it seems to be most natural to build the inference on the channel frequency response (CFR), which is estimated in regular intervals by PLC modems anyway. Grid diagnostics would thus be a by-product of the conventional modem operation, and the additions required for online monitoring would reduce to software updates. We also note that such diagnostics need not replace but would be used in addition to well-established maintenance and testing methods [9].

One key question to ask is whether cable aging can be detected via PLC transmission. While it is fairly obvious that changing cable characteristics lead to variations in the CFR for PLC signals, it remains unclear whether these variations are significant enough and indicative of cable degradations. The previous works [6], [7] considered isolated cable pieces, modified specific cable parameters in a section of the cable, and observed variations in the CFR. Compared to these, we make three important contributions. First, we attempt to apply a faithful model for cable aging based on the physical processes due to which cable degradation occurs. To this end, we consider the deterioration of the cable insulation due to a phenomenon called water treeing, which is a frequent cause of premature failure of medium-voltage cables with polyethylene dielectric insulation [10]. Water treeing is a degradation mechanism for polymers that occurs in serviced-aged cables and permanently damages the insulation, see e.g. [11], [12]. We use results presented for water treeing in cross-linked polyethylene (XLPE) medium-voltage cables in [13] that allow us to analyze the effects on cable parameters relevant for the PLC signal propagation. Secondly, we do not only consider a cable in isolation, but study the changes in the CFR due to water treeing when the cable is part of a network with varying load impedances. The classification of the source of CFR variations is accomplished in an automated fashion through the application of a support vector machine, which is our third contribution. Overall, our results are encouraging that broadband PLC based monitoring of cable aging is feasible. Thus, this work makes a step toward understanding and realizing such a grid diagnostics task.

The remainder of this paper is organized as follows. We briefly review the basics of transmission line modeling in Section II. The modeling of water treeing is described in Section III, and its impact on the signal transfer characteristics is analyzed in Section IV. The automated classification process is presented in Section V, before the final remarks in Section VI.

II. Preliminaries

The basic premise of our approach is that frequency responses of PLC channels reveal insight into the state of cable aging. To investigate this hypothesis, we require a reasonably faithful representation of CFRs as a function of cable characteristics. For this purpose, we apply the deterministic modeling approach assuming that PLC signals have a quasi-transverse electromagnetic (TEM) structure. This approach requires the following two basic steps.

a) Computation of Per-Unit-Length (PUL) Parameters: The TEM wave propagation characteristics of power lines are specified through the PUL parameters. Assuming $n+1$ conductors, we can set up the $n \times n$ PUL matrices $\boldsymbol{R}$, $\boldsymbol{G}$, $\boldsymbol{C}$, and $\boldsymbol{L}$, whose elements represent PUL resistances, conductance, capacitance and inductance as given in [14, Eq. (3.11), (3.12), (3.23), (3.24)]. There are generally no closed-form expressions for the $\boldsymbol{G}$, $\boldsymbol{C}$ and $\boldsymbol{L}$ parameters when considering closely spaced conductors with inhomogeneous surroundings. We thus apply the tool developed in [15] to compute PUL parameters. It is based on the numerical computation of a complex-valued capacitance matrix, from which $\boldsymbol{G}$ and $\boldsymbol{C}$ can be obtained, and the computation of the PUL capacitance matrix for free space as surrounding medium, from which $\boldsymbol{L}$ follows. For details we refer to [15].

b) Computation of Frequency Responses: From the PUL parameters we obtain the characteristic impedance and admittance matrices $\boldsymbol{Z}$ and $\boldsymbol{Y}$ for power lines. Together with the specification of impedances for loads connected to the power line network, we can determine the voltage transfer function, i.e., the CFR, between two points in the network using for example the impedance carry-back method described in [16].

With the above-summarized methodology in place, in the following we focus on the modeling of cable aging and its effects on PUL and eventually PLC channel characteristics.

III. Modeling of Water Treeing in XLPE Cables

In this section, we describe the influence of water treeing on the dielectric parameters of XLPE medium voltage cables.

A. XLPE Medium Voltage Cables

XLPE is a popular insulation material for both transmission and distribution systems as it offers several advantages in terms of cost, environmental impact, maintenance requirements and reliability [12]. The structure of a typical medium voltage XLPE multi-core cable is depicted in Figure 1. Each core consists of stranded, circular wires and is coated by an inner semi-conducting layer, which is followed by an XLPE insulation (blue), a tape of conductive material and a screen of copper wires. Further, the insulated cores are embedded in an extruded sheath and the cable is finally surrounded by an outer polyvinylchlorid (PVC) jacket (red) [17].

B. Water Treeing

Electrical and mechanical stress can affect and weaken the insulation of a power cable leading to a phenomenon called water treeing. According to [18], water treeing can be

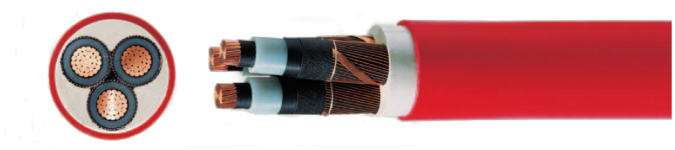

Fig. 1: XLPE multi-core cable N2XSEY from HELUKABEL® [17]

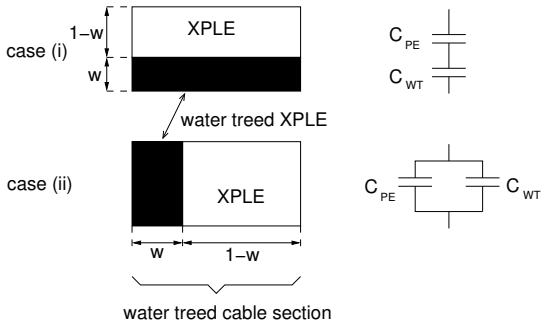

Fig. 2: Representation for water treed cables (left) and associated models for PUL parameters (right), following [13].

defined as an intrinsic degradation mechanism for polymers. Due to the combination of a varying electric field and a water electrolyte, a diffuse structure consisting of strings of water-filled microvoids of about 1 μm in diameter can rise in the insulation material. These tree-like structures (see [12, Fig. 4], [10, Fig. 5], [13, Figs. 6.4 and 6.7]) of moistures can penetrate the entire insulation and grow along the cable axis.

C. Influence on Cable Parameters

The impact of water treeing on the dielectric properties of medium voltage XLPE cables has been investigated in [13]. The author describes two manifestations of water trees, namely (i) water trees that are relatively short with respect to the thickness of the insulation and (ii) water trees that go through the entire insulation. These two cases are illustrated in Figure 2 (left), where the parameter $0 \leq w \leq 1$ determines the severity of water treeing. The associated models for the PUL capacitances are shown as parallel and series compositions on the right side of Figure 2.

The relative permittivity for the water treed region is given as [13, Eq. (6.2)] (from [19])

$$\epsilon_{\mathrm{WT}} = \epsilon_{\mathrm{PE}} \left(1 + \frac{q_{\mathrm{w}}(\epsilon_{\mathrm{w}} - \epsilon_{\mathrm{PE}})}{\epsilon_{\mathrm{PE}} + D(1-q_{\mathrm{w}})(\epsilon_{\mathrm{w}} - \epsilon_{\mathrm{PE}})} \right), \quad (1)$$

where $\epsilon_{\mathrm{w}} = 81 - \mathrm{j}\frac{\sigma_{\mathrm{w}}}{2\pi f \epsilon_0}$, σ_{w} is the water conductivity, and ϵ_{PE} is the complex relative permittivity of non-degraded XLPE. The parameter D models the shape of the microvoids and q_{w} is the absolute water content in the water treed region.

Depending on the water treeing scenario shown in Figure 2, the effective permittivity for a water treed cable section is obtained as

$$\text{case (i):} \quad \epsilon_{\mathrm{WT,t}} = \frac{1}{w/\epsilon_{\mathrm{WT}} + (1-w)/\epsilon_{\mathrm{PE}}} \quad (2)$$

or

$$\text{case (ii):} \quad \epsilon_{\mathrm{WT,t}} = w\epsilon_{\mathrm{WT}} + (1-w)\epsilon_{\mathrm{PE}} \,. \quad (3)$$

TABLE I: Electrical and geometric cable parameters.

ϵ_0	$\epsilon_{\mathrm{r,PE}}$	$\epsilon_{\mathrm{r,PVC}}$	σ_{Cu}
$8.854 \cdot 10^{-12}$ F/m	$2.3 - \mathrm{j}0.001$	$4.0 - \mathrm{j}0.120$	$5.96 \cdot 10^{7}$ S/m

core radius	number of strands	strand radius	XLPE insulation thickness	PVC insulation thickness	outer cable radius
3.99 mm	19	0.915 mm	2.5 mm	3.4 mm	25 mm

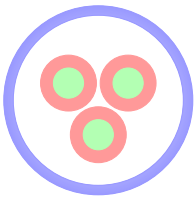

Fig. 3: Cross section of test cable.

For results shown in the following sections, we consider the scenario that water trees that go through the entire insulation, which has been observed in [13] for service-aged cable samples. We thus use (3) in the following.

IV. Impact of Water Treeing on Channel Transfer Characteristics

We apply the results for the permittivity above to quantify the impact of water treeing on the channel characteristics of XLPE cables, considering the frequency range generally used by PLC signals.

A. Test Setup

We consider a three core XLPE insulated cable N2SXEY as shown in Figure 1. The electric and geometric parameters are summarized in Table I. The dielectric parameters are obtained from [20, p. 794], the geometric parameters are calculated using the data provided in [17] and [21].

Figure 3 depicts the cable model. Each core (green color) consists of 19 stranded round wires. The inner XLPE insulation is shown in red and the outer PVC insulation is blue. We omit the semi-conducting coating, the copper screen and the extruded sheath in our model, which simplifies the numerical computation of the PUL parameters and is not expected to alter the results notably.

For the following results, we assume that $w = 0.2$ in (3), and we consider the frequency range from 100 kHz to 35 MHz, which covers the band mainly used by broadband PLC.

B. Impact on PUL Parameters

Expressing permittivities in terms of real and imaginary parts, i.e., $\epsilon = \epsilon' + \mathrm{j}\epsilon''$, Figure 4 shows ratio of the real and the imaginary parts of the complex permittivities of a water treed and an intact cable as a function of frequency f. We observe that the ratio deviates from one, indicating the effect of water treeing. Furthermore, we note that the ratios are frequency dependent, due to the fact that the relative permittivity ϵ_{WT} changes with frequency. This is different from [6] investigating cable degradation, which stipulated a frequency independent complex relative permittivity without consulting a physical model for degradation.

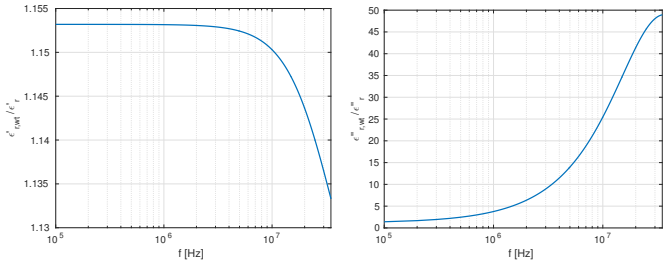

(a) Real part (b) Imaginary part

Fig. 4: Ratio of the complex permittivities of a water treed and an intact cable.

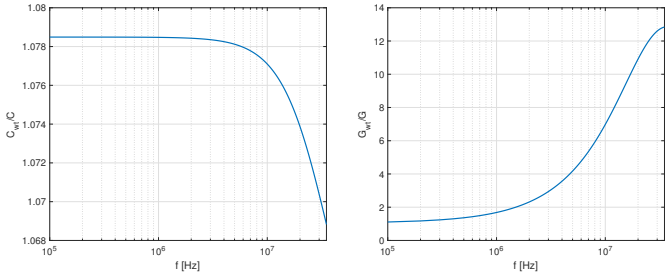

(a) Capacitance ratio $C_{\mathrm{WT},11}/C_{11}$ (b) Conductance ratio $G_{\mathrm{WT},11}/G_{11}$

Fig. 5: Ratios of the PUL capacities and conductances of a water treed and an intact cable.

We now use the permittivity results for the computation of the PUL parameters of the N2SXEY cable via the open-source tool presented in [15]. The PUL parameters affected by permittivity are the capacitance $\boldsymbol{C}$ and conductance $\boldsymbol{G}$, which for the three-conductor cable considered here are 2×2 matrices. Figure 5 show the ratios of the PUL capacities C_{11} and conductances G_{11} of a water treed and an intact cable, respectively. Comparing the curves in Figure 5 with those in Figure 4 we observe that the frequency characteristics of the capacity and the conductance follow the real and imaginary part of the complex permittivity, respectively, which is a result of [15, Eqs. (8), (9)]. It can also be seen that the relative changes in PUL conductance due to water treeing are more pronounced than those for PUL capacitance.

C. Impact on Channel Frequency Response

To illustrate the impact of the frequency dependent PUL parameters on the CFR, we consider the setup shown in Figure 6. It consists of a 20 m XLPE cable terminated on both sides by 50 Ω impedances.

The direct and cross-talk CFRs for both intact and water treed cable are shown in Figure 7 and 8, respectively. For this comparison, it is assumed that the entire cable is affected by water treeing. The direct CFR refers to the path from the inserted voltage V to the voltage across the first port terminated by R_{10}^{RX}, while the crosstalk is from V to the second port terminated with R_{20}^{RX}.

We observe from Figures 7 and 8 that water treeing causes a frequency shift in the CFR that grows with increasing fre-

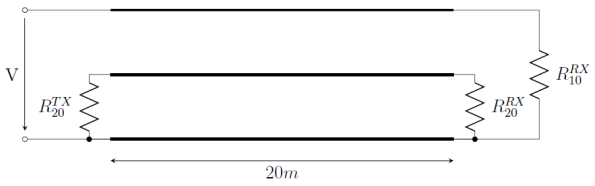

Fig. 6: Transmission line setup for frequency response test.

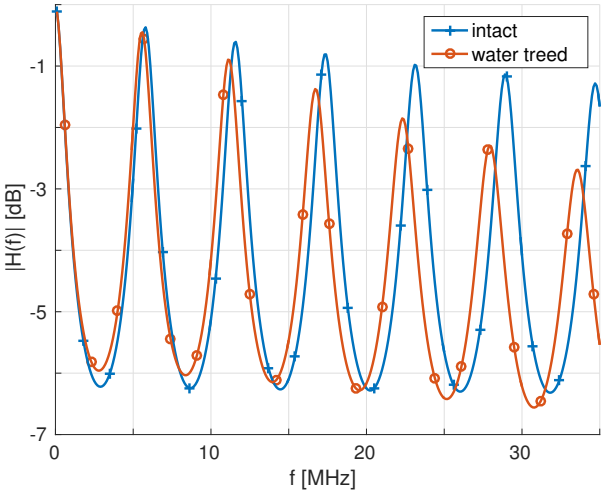

Fig. 7: Magnitude of direct CFR for intact and water treed cable for the setup in Figure 6.

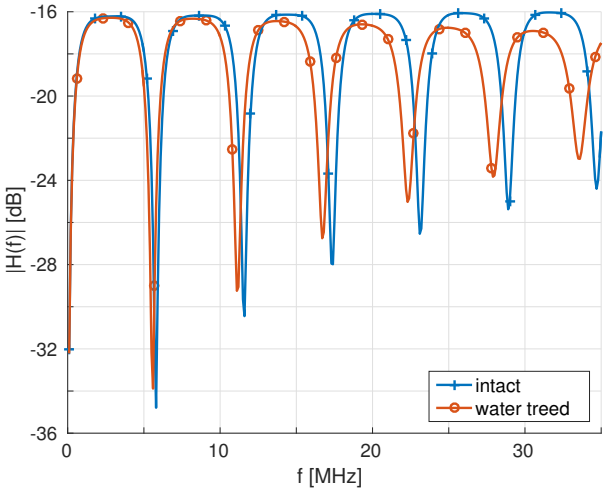

Fig. 8: Magnitude of cross-CFR for intact and water treed cable for the setup in Figure 6.

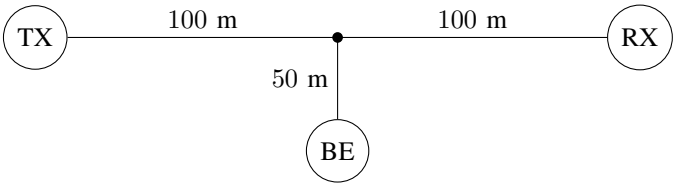

Fig. 9: Sample network to study feature extraction.

quency. This is due to the changes in the PUL capacitance with water treeing. Furthermore, signal attenuation is increasing faster for higher frequencies for the water treed cable. This can be attributed to the increased conductance for the water treed cable.

Overall, the numerical analysis in this section suggests that water treeing leads to noticeable changes in the CFR as experienced in a PLC system. This provides a basis for the machine learning classification presented in the next section.

V. Automated Diagnostics

We finally turn to the problem of identifying whether a cable has been affected by water treeing or not. For this purpose, we apply a binary classifier in the form of the support vector machine (SVM) [22]. For effective operation of the SVM, the judicious choice of features is required.

A. Feature Extraction

The SVM separates instances into classes based on comparing their combined characteristics with a threshold. It is crucial to prepare the data in such a way that meaningful features can be obtained. For the problem at hand, it has to be ensured that the chosen features allow to distinguish between water treed and intact cables. In addition to that, other influences on a PLC network have to be considered, especially the variation of load conditions.

In order to gain insight into the differentiation between the effects that arise from water treeing and from varying loads, the frequency response of the sample network shown in Figure 9 is considered. It is built on the three-conductor XLPE cable which has been analyzed in Section IV. We evaluate the direct transfer function between two conductors. The impedances between the unused conductor and the reference conductor are set to $R_{20}^{\mathrm{TX}} = R_{20}^{\mathrm{RX}} = 50\ \Omega$, see Figure 6. Based on this simple network, we can test the following four scenarios:

1) Both receiver (RX) and branch endpoint (BE) are terminated with 50 Ω and all wires are intact,
2) both RX and BE are terminated with 50 Ω and a section of 60 m between the branch point and the receiver is water treed,
3) both RX and BE are terminated with 20 Ω and all wires are intact, and
4) both RX and BE are terminated with 20 Ω and a section of 60 m between the branch point and the receiver is water treed.

Figure 10 shows the magnitude CFR for the four test scenarios. As already discussed in Section IV-C, water treeing causes a slight frequency shift toward lower frequencies. However, the effect caused by different load conditions is significantly more pronounced than the changes due to the water treed cable section, even though water treeing is quite progressed in the cable, as already 60 % of the second leg between TX and RX are assumed to be affected. These results indicate the difficulty of the desired classification task.

In order to render the effect of water treeing more visible, we normalize each measured frequency response with a reference function. For the considered scenarios, we use the

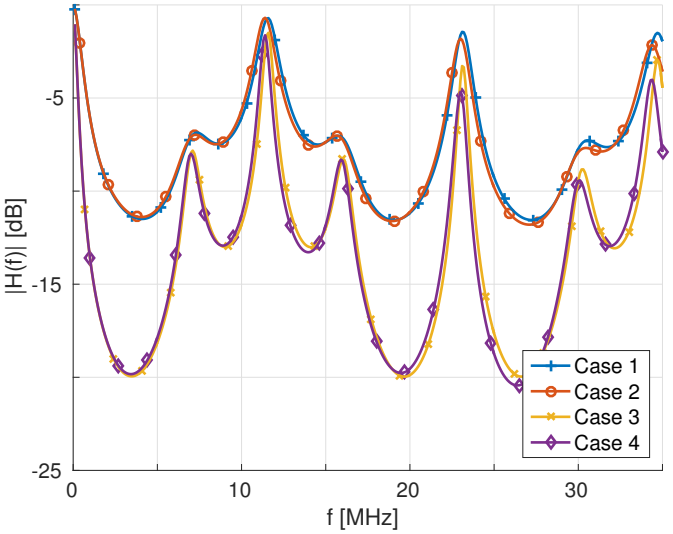

Fig. 10: Magnitude CFR for the setup in Figure 9 and four different test scenarios.

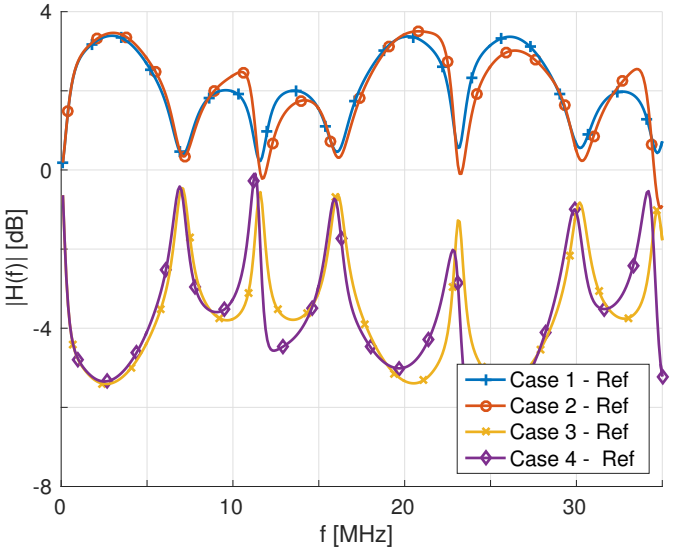

Fig. 11: Magnitude normalized CFR for the setup in Figure 9 and four different test scenarios.

frequency response between TX and RX when receiver and branch endpoint are terminated with a 35 Ω impedance and all cable sections are intact. Figure 11 shows the results from Figure 10 when applying this normalization. As expected, the different load conditions are still clearly separable and dominate the changes in measured responses. In particular, the loads have a significant effect on peaks and notches of the frequency response. A statistical measure that captures such characteristics is the kurtosis. Furthermore, for both the 50 Ω termination (cases 1 and 2) and the 20 Ω termination (cases 3 and 4) the differences between water treed and intact scenarios become now more distinct in that the curves are differently lopsided. This fact can be represented by the skewness, which is a statistical measure of the asymmetry.

We thus consider the following features as input to the SVM:

(A) Skewness and kurtosis of magnitude and phase of the CFR.
(B) Skewness and kurtosis of magnitude and phase of the normalized CFR.

B. *Classification Results*

Continuing with the test network shown in Figure 9, a set of 1000 CFRs is generated to train the SVM. The first 500 realizations represent the network with all cables intact. For the second 500 samples a water treed section between branch point and RX is introduced, which expands gradually from 0 m to 100 m. In order to analyze the impact of the reference function and loads, we consider three scenarios:

1) the loads at RX and BE are chosen uniformly at random in the range of $[0, 50]$ Ω, the loads for the reference function are set to 50 Ω,
2) the loads at RX and BE are chosen uniformly at random in the range of $[0, 50]$ Ω, the loads for the reference function are set to 10 Ω,
3) the loads at RX and BE are chosen uniformly at random in the range of $([0, 50] + \mathrm{j}[-50, 50])$ Ω, the loads for the reference function set to $(50 + \mathrm{j}50)$ Ω.

The classification performance is measured in terms of the detection rate

$$P_{\mathrm{det}} = \Pr(\text{water treeing detected}|\text{water treeing occurred}) \tag{4}$$

and the false alarm rate

$$P_{\mathrm{fa}} = \Pr(\text{water treeing detected}|\text{no water treeing occurred}) \,. \tag{5}$$

For the performance evaluation, the classifier is tested with another set of 500 CFRs. One half of the samples represent a network with intact cables, the other half is generated with a 40 m long water treed section between the branch point and the receiver.

Table II shows the results for detection rate and false alarm rate for the above defined feature combinations (A) and (B) and load configurations (1) to (3). Comparing the two feature combinations, we note that normalizing to a reference function improves both detection and false alarm rate. Considering load configurations (1) and (2) indicates some impact of how the loads for the reference function are chosen. As not unexpected, the classification results for the more complex scenario (3) are worse than for scenarios (1) and (2), which can be explained with more variability of CFRs due to the introduction of complex-valued loads.

Finally, we consider the detection and false alarm rate performance as a function of the length of the water treed section in Figure 12. The length of water treed section increases from 0 m to 100 m in steps of 5 m, and for each length 250 frequency response samples for intact cables and 250 samples for water treed cables are generated. The false alarm rate is independent on the length of the water treeing, and thus an average of all results is shown in Figure 12. Load configuration (3) and feature combination (B) are applied. We observe that while the false alarm rate is around 15%, the detection rate improves with expanding water treeing in the cable. For a

TABLE II: Classification performance in terms of detection and false alarm rates for different feature combinations and load configurations. 40 m water treed cable section.

		feature combination			
		(A)		(B)	
		P_{det}	P_{fa}	P_{det}	P_{fa}
load conf.	(1)	0.92	0.04	1.00	0.00
	(2)	0.87	0.02	1.00	0.00
	(3)	0.67	0.28	0.94	0.15

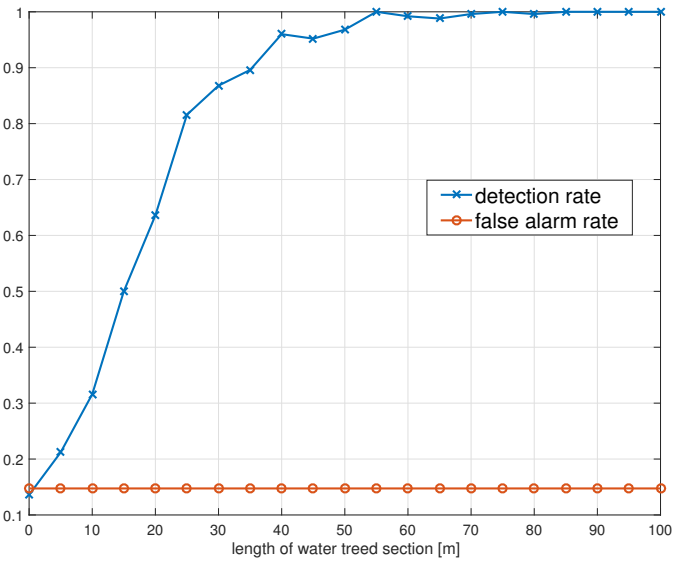

Fig. 12: Detection and false alarm rates as functions of the length of the water treed section.

length of about 30 m and more, the detection rate is above 90%, suggesting a fairly successful classification.

VI. Conclusions

In this paper, we have investigated the use of broadband PLC for an application of grid diagnostics, namely cable aging. We have applied a meaningful model for the degradation of service-aged cables in the form of water treeing, and analyzed how this impairment affects PUL cable parameters. Our numerical tests for an isolated cable segment have shown noticeable changes to the channel frequency response measurable with broadband PLC modems due to the presence of water treeing. These become however masked by load variations in more complicated networks. We therefore devised features that enabled an SVM classifier to relatively reliably differentiate between variations caused by cable aging and those due to load changes. As a critical note we remark that in our model we differentiated between an intact and an $X\%$ degraded cable using a fixed reference channel. In a practical setting, cable aging occurs over time, and a more suitable approach than binary classification may be to infer the extent of degradation. Hence, we consider the presented classification only as a first step toward the objective of online monitoring.

References

[1] L. Lampe, A. Tonello, and T. Swart, Eds., *Power Line Communications: Principles, Standards and Applications from Multimedia to Smart Grid*, 2nd ed. UK: John Wiley & Sons Ltd, Jun. 2016.

[2] V. Taylor and M. Faulkner, "Line monitoring and fault location using spread spectrum on power line carrier," *IEE Proceedings-Generation, Transmission and Distribution*, vol. 143, no. 5, pp. 427 –434, Sep. 1996.

[3] A. N. Milioudis, G. T. Andreou, and D. P. Labridis, "Enhanced protection scheme for smart grids using power line communications techniques — Part II: Location of high impedance fault position," *IEEE Trans. Smart Grid*, vol. 3, no. 4, pp. 1631–1640, 2012.

[4] M. Ahmed and L. Lampe, "Power line communications for low-voltage power grid tomography," *IEEE Trans. Commun.*, vol. 61, no. 12, pp. 5163–5175, Dec. 2013.

[5] T. Erseghe, S. Tomasin, and A. Vigato, "Topology estimation for smart micro grids via powerline communications," *IEEE Trans. Signal Processing*, vol. 61, no. 13, pp. 3368–3377, Jul. 2013.

[6] F. Yang, W. Ding, and J. Song, "Non-intrusive power line quality monitoring based on power line communications," in *IEEE International Symposium on Power Line Communications and Its Applications (ISPLC)*, Johannesburg, South Africa, Mar. 2013, pp. 191–196.

[7] A. M. Lehmann, K. Raab, F. Gruber, E. Fischer, R. R. Müller, and J. Huber, "A diagnostic method for power line networks by channel estimation of PLC devices," in *IEEE Intl. Conf. on Smart Grid Commun.*, Sydney, Australia, Nov. 2016.

[8] A. Pinomaa, J. Ahola, A. Kosonen, and T. Ahonen, "Diagnostics of low-voltage power cables by using broadband impedance spectroscopy," in *European Conference on Power Electronics and Applications (EPE'15 ECCE-Europe)*, Sep. 2015, pp. 1–10.

[9] P. Gill, *Electrical Power Equipment Maintenance and Testing*, 2nd ed. CRC Press, 2008.

[10] W. Shu, J. Guo, and S. A. Boggs, "Water treeing in low voltage cables," *IEEE Electrical Insulation Magazine*, vol. 29, no. 2, pp. 63–68, Mar. 2013.

[11] R. Patsch and J. Jung, "Water trees in cables: generation and detection," *IEE Proceedings - Science, Measurement and Technology*, vol. 146, no. 5, pp. 253–259, Sep. 1999.

[12] H. Orton, "History of underground power cables," *IEEE Electrical Insulation Magazine*, vol. 29, no. 4, pp. 52–57, Jul. 2013.

[13] G. Mugala, "High frequency characteristics of medium voltage XLPE power cables," Ph.D. dissertation, KTH Royal Institute of Technology, Stockhol, Sweden, Nov. 2005.

[14] C. R. Paul, *Analysis of multiconductor transmission lines*, 2nd ed. John Wiley & Sons, 2008.

[15] F. Gruber and L. Lampe, "On PLC Channel Emulation via Transmission Line Theory," in *IEEE International Symposium on Power Line Communications and Its Applications (ISPLC)*, Austin, TX, USA, Mar. 2015. [Online]. Available: http://www.ece.ubc.ca/~lampe/MIMOPLC/

[16] F. Versolatto and A. Tonello, "An MTL theory approach for the simulation of MIMO power-line communication channels," *IEEE Trans. Power Delivery*, vol. 26, no. 3, pp. 1710–1717, Jul. 2011.

[17] HELUKABEL®, "Medium VoltagePower Cables," http://mdmetric.com/prod/helukabel/N.Medium%20Voltage%20Power.pdf, p. N 21, 04.04.2016.

[18] J. Fothergill, A. Eccles, J. Houlgreave, and L. Dissado, "Water tree inception and its dependence upon electric field, voltage and frequency," *IEE Proceedings A - Science, Measurement and Technology*, vol. 140, no. 5, pp. 397 – 403, 1993.

[19] F. Stucki, "Dielectric properties and I-V-characteristics of single water trees," in *IEEJ Workshop on Electrical Insulation*, Nagoya, Japan, Sep. 1993.

[20] W. Titow, *PVC plastics: properties, processing, and applications*. London, New York: Elsevier Applied Science, 1990.

[21] Baude, "Structure of stranded wires in accordance with VDE 0295 and amplified," http://baude.com/fileadmin/content/Download/structure-of-stranded-wires-in-accordance-with-vde0295.pdf, 04.04.2016.

[22] C. M. Bishop, *Pattern Recognition and Machine Learning (Information Science and Statistics)*. Secaucus, NJ, USA: Springer-Verlag New York, Inc., 2006.